

# Push-Pull Stiff-Stilbene: Proton-Gated Visible-Light Photoswitching and Acid-Catalyzed Isomerization

David Villarón,<sup>[a]</sup> Nol Duindam,<sup>[a]</sup> and Sander J. Wezenberg\*<sup>[a]</sup>

*Dedicated to the memory of François Diederich*

**Abstract:** Donor-acceptor substituted stiff-stilbene is shown to undergo isomerization induced by visible light avoiding the need for harmful UV light. This visible-light photoswitching is inhibited by protonation of the dimethylamino-donor unit, disrupting the push-pull character and thus, gating of the photochromic properties is allowed by acid/base addition. Remarkably, the addition of a mild acid also triggers fast thermal back-isomerization, which is unprecedented for stiff-stilbene photoswitches usually having a very high energy barrier for this process. These combined features offer unique orthogonal control over switching behavior by light and protonation, which is investigated in detail by <sup>1</sup>H NMR and UV/Vis spectroscopy. In addition, TD-DFT calculations are used to gain further insight into the absorption properties. Our results will help elevating the level of control over dynamic behavior in stiff-stilbene applications.

Among molecular photoswitches,<sup>[1]</sup> stiff-stilbene is emerging as a powerful tool to construct dynamic functional molecular systems.<sup>[2]</sup> While originally designed as a prototype for gaining insight into stilbene photoisomerization,<sup>[3]</sup> its current applications range from the fields of molecular receptors,<sup>[4]</sup> supramolecular polymers,<sup>[5]</sup> and catalysis,<sup>[6]</sup> to lipid bilayer transport.<sup>[7]</sup> Stiff-stilbene has two thermally stable states (P-type photoswitch), high structural rigidity, an efficient photoisomerization process, and undergoes a large geometrical change upon isomerization. However, despite these advantageous properties, they rely on activation by high-energy UV light causing material degradation and limiting potential application in biology.

The need for activation by UV light is a general drawback of most organic photoswitches and therefore, several strategies have been developed to red-shift their excitation wavelengths to the visible-light range.<sup>[8]</sup> The creation of “push-pull” systems by attachment of electron-donating and -withdrawing groups has, for instance, proven successful for azobenzene switches<sup>[9]</sup> and overcrowded alkene-based molecular motors.<sup>[10]</sup> In addition to visible-light-induced switching, there is rapidly growing interest in the development of dual-stimuli responsive photochromic systems. For example, by gating the photochromic properties using redox processes,<sup>[11]</sup> ion binding,<sup>[12]</sup> acid/base,<sup>[13]</sup> or macrocyclic hosts that bind/thread the molecular photoswitch.<sup>[14]</sup> Furthermore, acid addition was found to elevate the thermal isomerization barrier of certain azobenzene derivatives<sup>[15]</sup> and conversely, was used to catalyze thermal ring-opening of diarylethene in order to release the energy stored in the photogenerated form.<sup>[16]</sup> Such dual-responsiveness offers an improved level of control over isomerization behavior and therefore, will likely lead to the development of more complex and sophisticated dynamic functions, as well as the improvement of molecular opto-electronic (memory) devices. Yet, orthogonality between the different stimuli, which is an essential prerequisite, remains highly challenging to achieve.<sup>[17]</sup>

Toward visible-light switching of stiff-stilbene, we decided to investigate the influence of donor-acceptor substituents on the photochromic properties. Therefore, compound (*E*)-1 containing a dimethylamino and cyano group in *para*-position to the double bond was synthesized.<sup>[18]</sup> Herein, we demonstrate that isomerization of **1** can be triggered by visible light (405/455 nm) and that reversible protonation of the dimethylamino-donor unit using mild acid/base allows gating of this process (Scheme 1). Moreover, the acid was found to catalyze thermally-activated *Z*→*E* back-isomerization and hence, by incorporating donor-acceptor substituents, unprecedented control over stiff-stilbene switching behavior is achieved.

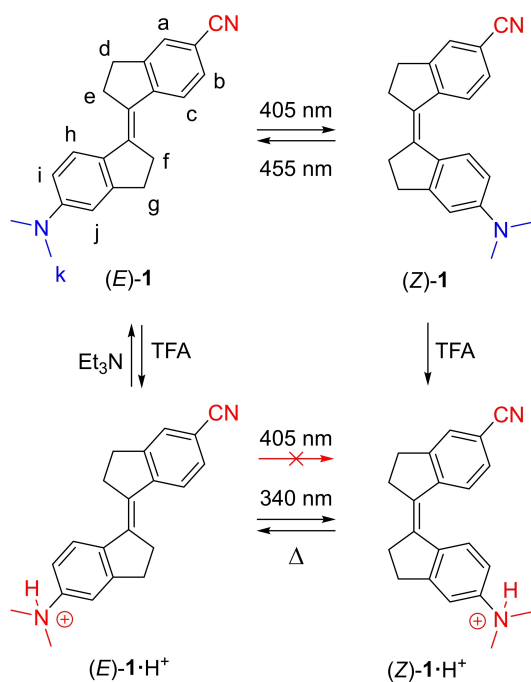
Desymmetrization of stiff-stilbene has previously been achieved through mixed McMurry<sup>[4d,f]</sup> and Barton-Kellogg<sup>[19]</sup> reactions. In 1992, Lapouyade and co-workers first described compound (*E*)-1, which was obtained via a mixed coupling of 5-bromo-1-indanone and 5-dimethylamino-1-indanone followed by cyanation using copper cyanide.<sup>[18]</sup> Unfortunately, when we attempted a mixed McMurry coupling with these indanones, only a trace amount of the desired heterocoupled product was observed in the <sup>1</sup>H NMR spectrum of the crude reaction mixture, which mainly consisted of 5,5'-dibromo-substituted stiff-stilbene (Figure S13 in the Supporting Information). Therefore, we

[a] D. Villarón, N. Duindam, Dr. S. J. Wezenberg  
Leiden Institute of Chemistry  
Leiden University  
Einsteinweg 55, 2333 CC Leiden (The Netherlands)  
E-mail: s.j.wezenberg@lic.leidenuniv.nl

Supporting information for this article is available on the WWW under <https://doi.org/10.1002/chem.202103052>

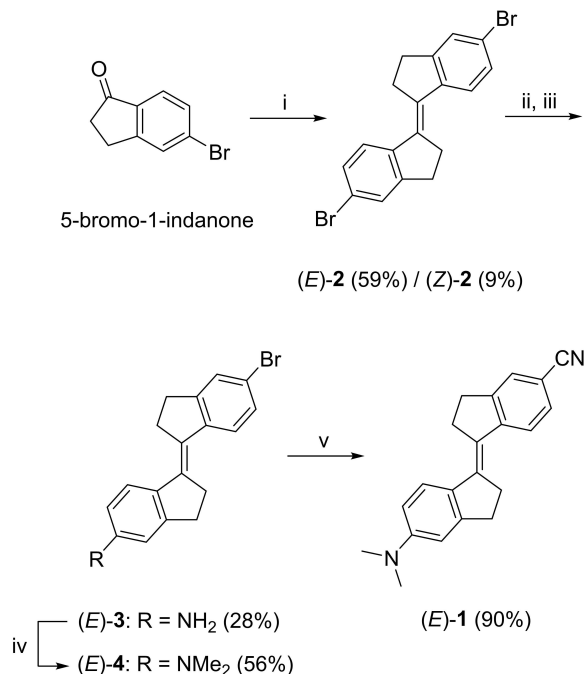
This article belongs to a Joint Special Collection dedicated to François Diederich.

© 2021 The Authors. Chemistry - A European Journal published by Wiley-VCH GmbH. This is an open access article under the terms of the Creative Commons Attribution License, which permits use, distribution and reproduction in any medium, provided the original work is properly cited.



**Scheme 1.** Light-induced and acid/base-controlled isomerization steps of donor-acceptor substituted stiff-stilbene **1**.

devised an alternative strategy for stiff-stilbene desymmetrization based on mono-functionalization of the 5,5'-dibromo product (see Scheme 2 and the Supporting Information for



**Scheme 2.** Synthesis of push-pull stiff-stilbene (*E*)-**1**: (i) Zn, TiCl<sub>4</sub>, THF, reflux; (ii) benzophenone imine, Pd(OAc)<sub>2</sub>, DPPF, NaOtBu, toluene, 90 °C; (iii) 2 M aqueous HCl, THF; (iv) MeI, K<sub>2</sub>CO<sub>3</sub>, DMF; (v) Zn(CN)<sub>2</sub>, tBuXPhos, tBuXPhos-Pd-G3, DMF/H<sub>2</sub>O (99:1 v/v). Note that only the (*E*)-isomer of **2** is drawn in the scheme for convenience.

synthetic details and characterization). First, McMurry homocoupling of 5-bromo-1-indanone afforded a mixture of (*E*)-**2** and (*Z*)-**2**. The (*E*)-isomer could be isolated by precipitation and was submitted to Buchwald-Hartwig amination to obtain monoamine (*E*)-**3**. Subsequent methylation using methyl iodide under basic conditions, followed by Pd-catalyzed cyanation using zinc cyanide, gave the desired push-pull stiff-stilbene (*E*)-**1**.

The photoisomerization properties of (*E*)-**1** were initially examined by UV/Vis spectroscopy in MeCN solution. The UV/Vis absorption spectrum (Figure 1 and Figure S14 in the Supporting Information) shows a maximum at  $\lambda = 398$  nm and is similar to the one reported by Lapouyade et al.<sup>[18]</sup> The overall absorption is considerably red-shifted with respect to unsubstituted stiff-stilbene ( $\lambda_{\text{max}} = 342$  nm, 324 nm, see Figure S23 in the Supporting Information)<sup>[3]</sup> revealing a smaller HOMO-LUMO gap. Irradiation with 405 nm light resulted in a decrease of the absorption maximum and a slight bathochromic shift, which can be ascribed to *E*→*Z* isomerization (Figure 1A).<sup>[2-7]</sup> Consecutive irradiation with shorter wavelengths (i.e., 385 nm and 365 nm) led to a slightly larger decrease in absorption, implying higher conversion toward the (*Z*)-isomer. The reverse UV/Vis spectral changes were observed when the sample was subsequently irradiated with 455 nm light, demonstrating that the (*E*)-isomer can be regenerated, albeit not quantitatively. In all cases, irradiation was continued until the absorption spectrum did not change further meaning that the photostationary states (PSS) had been reached. Importantly, the clear isosbestic point

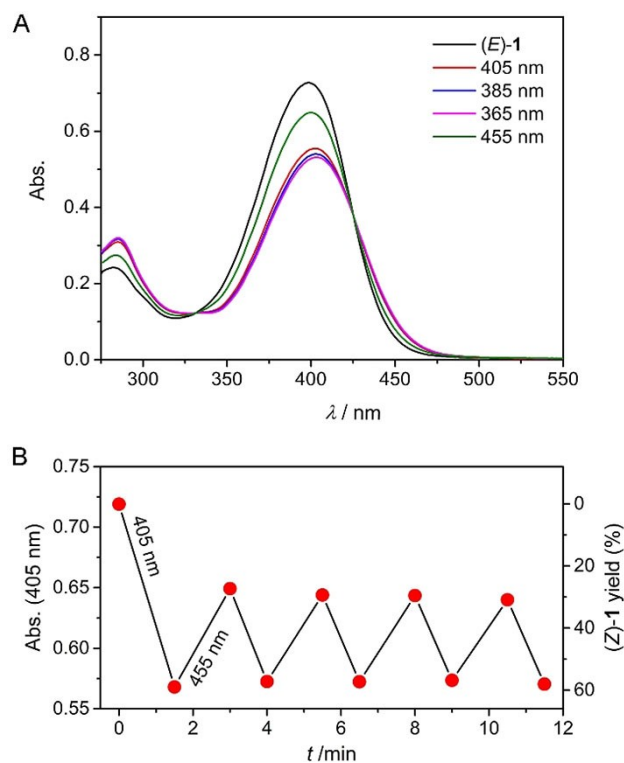


**Figure 1.** (A) UV/Vis spectral changes of (*E*)-**1** ( $2.5 \times 10^{-5}$  M in MeCN) upon sequential 405 nm, 385 nm, 365 nm, and 455 nm irradiation. (B) Plot of the change in absorption at  $\lambda = 405$  nm and (*Z*)-**1** amount upon multiple 405/455 nm switching cycles starting with (*E*)-**1** ( $2.5 \times 10^{-4}$  M in MeCN).

at  $\lambda = 425$  nm confirms unimolecular conversion (Figure S15 in the Supporting Information) and no signs of photodegradation were noted when 405/455 nm irradiation was repeated multiple times (Figure 1B). The quantum yield for 405 nm triggered  $E \rightarrow Z$  isomerization ( $\Phi_{E \rightarrow Z}$ ) was determined as  $27.2 \pm 0.26\%$  by using potassium ferrioxalate as actinometer (see Figures S16–17 and the Supporting Information for details). With the molar absorptivities and PSS ratio at 405 nm (see below), the quantum yield for the reverse process ( $\Phi_{Z \rightarrow E}$ ) was calculated as  $29.9 \pm 0.29\%$ .

Next, the  $E \rightarrow Z$  isomerization process was monitored with  $^1\text{H}$  NMR spectroscopy. Irradiation with either 405 nm or 365 nm light of a solution of (*E*)-1 in  $\text{MeCN-}d_3$  led to the appearance of a new set of  $^1\text{H}$  NMR signals, which were assigned to (*Z*)-1 (Figure 2 and Figure S18 in the Supporting Information). By relative integration, the  $\text{PSS}_{405}$  and  $\text{PSS}_{365}$  ratios were determined as 41:59 (*E/Z*) and 34:66 (*E/Z*), respectively, in line with the slightly larger UV/Vis absorption decrease when 365 nm light was used instead of 405 nm light. Using these PSS ratios and the change in absorbance at  $\lambda = 400$  nm, the  $\text{PSS}_{455}$  was estimated as 74:26 (*E/Z*) and the  $\text{PSS}_{385}$  ratio as 37:63 (*E/Z*) (Table S1 in the Supporting Information).

The absorption properties of (*E*)-1 were further investigated using TD-DFT calculations [B3LYP/6-31G(d,p), IEFPCM MeCN], which are in reasonable agreement with experimental data,<sup>[20]</sup> i.e.  $\lambda_{\text{max}}$  (exp) = 398 nm and  $\lambda_{\text{max}}$  (calcd) = 428 nm (see Figure S27 and the Supporting Information for details). The optical gap is significantly red-shifted with respect to unsubstituted stiff-stilbene (Figures S26–31 in the Supporting Information) and the  $S_0 \rightarrow S_1$  excitation was identified as a pure HOMO-LUMO  $\pi\text{-}\pi^*$  transition with a clear intramolecular charge-transfer component. That is, electron density migrates from the dimethylamino-donor to the cyano-acceptor upon excitation to the LUMO (Figure 3A). Furthermore, the LUMO displays antibonding character with regard to the central alkene illustrating that the double bond character is decreased in the excited state.

We then became interested to investigate the influence of dimethylamine protonation as it would disrupt the donor-acceptor character and hence, alter absorption - and usable excitation - wavelength. That would potentially allow protonated visible-light photoswitching. Indeed, TD-DFT calculations

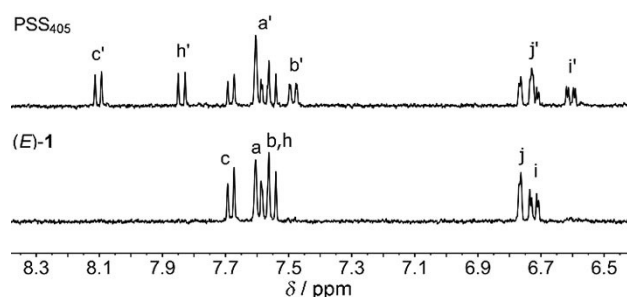


**Figure 2.** Aromatic region in the  $^1\text{H}$  NMR spectrum of (*E*)-1 (2.8 mM in  $\text{MeCN-}d_3$ , bottom) and the photostationary state mixture obtained upon 405 nm irradiation (top). The proton assignment is based on COSY and NOESY spectra, see Scheme 1 for the atom labeling.

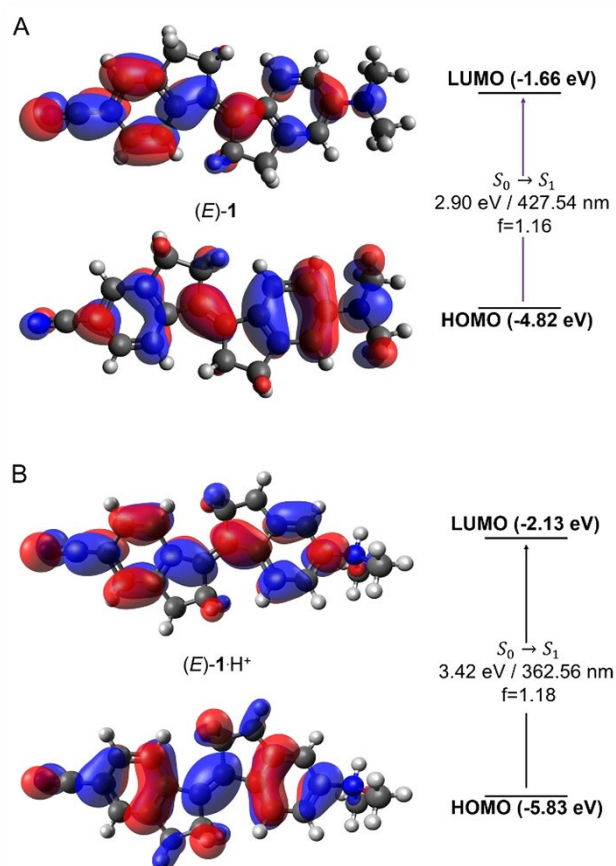


**Figure 3.** Visualization of the relevant frontier molecular orbitals alongside the predicted and dominating (> 99%)  $S_0 \rightarrow S_1$  HOMO-LUMO transitions ( $f$  = oscillator strength) for (A) (*E*)-1 and (B) (*E*)-1- $\text{H}^+$ . Please note that the  $S_0 \rightarrow S_1$  excitation energies (optical gaps) are shown on top of the arrows, between the HOMO and LUMO levels.

predicted a sharp blue-shift of 0.52 eV in the optical gap (i.e.  $S_0 \rightarrow S_1$  excitation energy) of (*E*)-1 upon protonation of the dimethylamino-donor unit, and inspection of the  $S_0 \rightarrow S_1$  transition revealed the loss of intramolecular charge transfer (see Figure 3B and Figure S29 in the Supporting Information).

In line with these predictions, addition of TFA to a solution of (*E*)-1 in MeCN led to a large hypsochromic shift, showing absorption maxima at much shorter wavelengths ( $\lambda_{\text{max}} = 361$  nm and 343 nm, Figure 4A and Figure S20 in the Supporting Information), with the shape of the absorption spectrum quite similar to unsubstituted stiff-stilbene (see Figure S23 in the Supporting Information). As the protonated species (*E*)-1- $\text{H}^+$  did not absorb light beyond  $\lambda = 400$  nm, irradiation with 405 nm light did not cause photoisomerization as evident from the absence of spectral changes. Nevertheless, irradiation of the protonated species with 340 nm light led to a decrease in absorption and a small bathochromic shift, indicating formation of the (*Z*)-1- $\text{H}^+$  isomer (Figure 4A and Figure S21 in the Supporting Information).

Whereas stiff-stilbene is known to have a very high energy barrier to thermal isomerization ( $\Delta^\ddagger G^\circ = 180$  kJ mol $^{-1}$  and  $t_{1/2} = 10^9$  years at 300 K),<sup>[21]</sup> to our surprise, the photogenerated (*Z*-

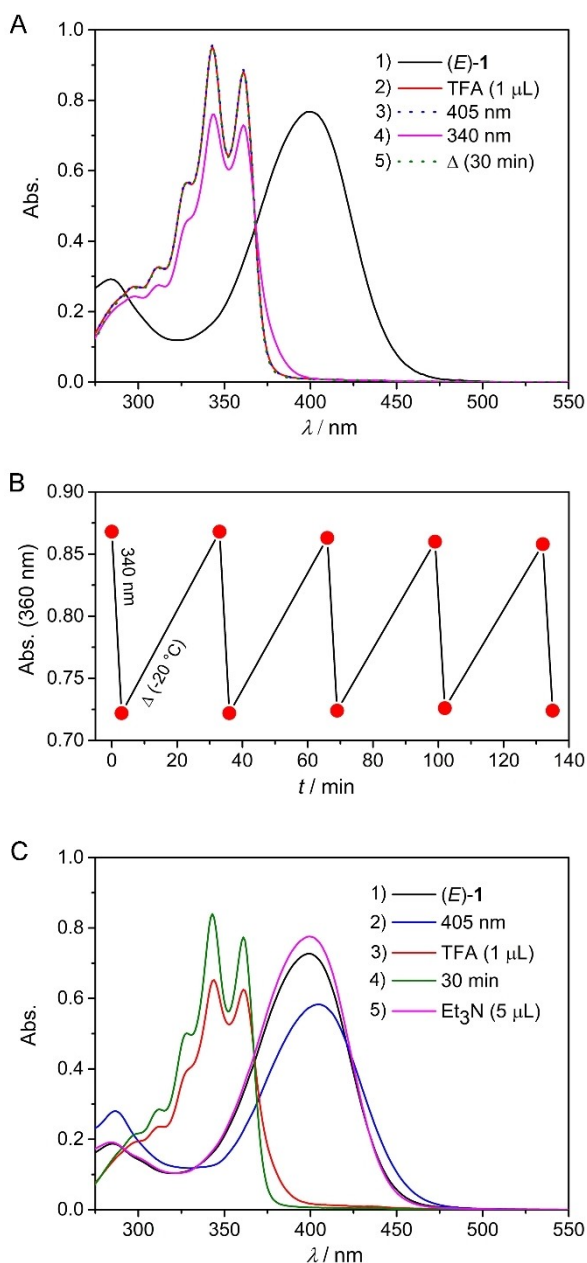


**Figure 4.** (A) UV/Vis spectral changes starting with (1)  $(E)$ -1 ( $2.5 \times 10^{-5}$  M in MeCN) recorded at  $-20^\circ\text{C}$  upon successive (2) addition of TFA (1  $\mu\text{L}$ , 0.05% v/v), (3) 405 and (4) 340 nm irradiation, and (5) equilibration for 30 min. (B) Plot of the change in absorbance at  $\lambda = 360$  nm upon sequential photo- and thermal isomerization steps. (C) Spectral changes starting with (1)  $(E)$ -1 upon successive (2) 405 nm irradiation, (3) TFA (1  $\mu\text{L}$ , 0.05% v/v) addition, (4) equilibration for 30 min, and (5)  $\text{Et}_3\text{N}$  (5  $\mu\text{L}$ , 0.25% v/v) addition.<sup>[24]</sup>

$1\text{-H}^+$  species spontaneously converted back to  $(E)\text{-1-H}^+$  as apparent from the recovery of the initial absorption band over time (Figure 4A and Figure S21 in the Supporting Information). A similar observation was made by  $^1\text{H}$  NMR spectroscopy where addition of TFA to a  $\text{PSS}_{365}$   $E/Z$  mixture led to rapid formation of  $(E)\text{-1-H}^+$  (see Figure S25 in the Supporting Information). These photo- and thermal isomerization steps could be repeated several times without signs of fatigue (Figure 4B). Importantly, under similar conditions, unsubstituted stiff-stilbene did not

show such acid-catalyzed isomerization behavior (Figure S23 in the Supporting Information) and moreover, only a minor change in  $\text{PSS}_{405}$   $(E)\text{-1}/(Z)\text{-1}$  ratio was noted in the absence of TFA for a sample that stood in the dark for 24 h (Figure S19 in the Supporting Information).

Acid-catalyzed  $Z \rightarrow E$  isomerization of stilbene has been known since long time, but requires very strong concentrated acid (50–60%  $\text{H}_2\text{SO}_4$ ).<sup>[22]</sup> The proposed mechanism involves double bond protonation to generate a carbenium ion intermediate, which is the rate-limiting step. Very recently, norbornene-fused stilbene was reported to isomerize under much milder conditions, i.e., in the presence of TFA the reaction was completed within 2 h at rt in  $\text{CH}_2\text{Cl}_2$  whereas it took several days in MeCN.<sup>[23]</sup> Also here a carbenium ion intermediate was suggested. In the present case, by determining the rate constant for conversion of  $(Z)\text{-1-H}^+$  into  $(E)\text{-1-H}^+$  at  $-20^\circ\text{C}$  using the absorption decay at 375 nm (see Figure S22 in the Supporting Information), we calculated a half-life ( $t_{1/2}$ ) at this temperature of 20.7 s, corresponding to a Gibbs free energy barrier ( $\Delta^\ddagger G^\circ$ ) of 68.8  $\text{kJ mol}^{-1}$ . TFA-mediated  $Z \rightarrow E$  isomerization proceeds thus very rapidly at this low temperature. Protonation of the double bond is tentatively predicted to play an important role here as well, however, the precise mechanism and the effect of other electron-donating and -withdrawing groups still need further investigation.

The serendipitous discovery of this acid-catalyzed  $Z \rightarrow E$  isomerization allows orthogonal switching by light and protonation as illustrated in Scheme 1. While the conversion of  $(Z)\text{-1}$  back into  $(E)\text{-1}$  is not quantitative when 455 nm irradiation is used ( $\text{PSS}_{455} = 74:26$   $E/Z$ ), the  $(E)$ -isomer can be fully regenerated by sequential protonation and deprotonation as demonstrated in Figure 4C. In short, by starting with a solution of  $(E)\text{-1}$ , initial 405 nm irradiation led to an absorption decrease as a result of the formation of  $(Z)\text{-1}$ . When then TFA was added to the  $\text{PSS}_{405}$   $E/Z$  mixture, the whole absorption spectrum became blue-shifted because of dimethylamine protonation and resulting loss of donor-acceptor character. The absorption increase that followed by letting the solution stand for 30 min revealed thermal conversion of  $(Z)\text{-1-H}^+$  into  $(E)\text{-1-H}^+$ . Final deprotonation using  $\text{Et}_3\text{N}$  gave back the UV/Vis absorption spectrum of the initial  $(E)$ -isomer (which slightly changed in the presence of this base)<sup>[24]</sup> and thus, completed the isomerization cycle. Importantly, the addition of acid can efficiently release the (visible light) energy stored in the photogenerated  $(Z)$ -form. In addition and as shown above, the  $(Z)\text{-1-H}^+$  species is alternatively accessible through TFA addition to  $(E)\text{-1}$  followed by 340 nm irradiation while 405 nm irradiation did not have any effect here. Visible-light-triggered isomerization can thus be switched on/off by using  $\text{Et}_3\text{N}$  and TFA, i.e. the photochromic properties are gated by acid/base.

In summary, we have synthesized a donor-acceptor substituted stiff-stilbene via a newly developed desymmetrization method based on mono-functionalization. This stiff-stilbene can be isomerized by visible light (405/455 nm) avoiding the need for harmful UV light, which is normally used to induce this process. The donor-acceptor character – and with that the visible light absorption – is lost by protonation of the dimeth-



ylamino-donor by using acid and is restored by treatment with base, offering proton-gated visible-light excitation. Remarkably, unprecedented TFA-catalyzed thermal  $Z \rightarrow E$  isomerization was observed, while the energy barrier to this process is known to be very high for unsubstituted stiff-stilbene.<sup>[21]</sup> This acid-catalyzed process would permit the use as a T-type photoswitch in “out-of-equilibrium” systems<sup>[25]</sup> and moreover, the orthogonal light and acid/base responsiveness will offer higher levels of control in materials and biological applications.<sup>[2]</sup>

## Acknowledgements

Financial support from the European Research Council (ERC Starting Grant no. 802830 to S.J.W.) is gratefully acknowledged.

## Conflict of Interest

The authors declare no conflict of interest.

**Keywords:** molecular switches · photochromism · proton gating · push-pull systems · stiff-stilbene

- [1] a) B. L. Feringa, *J. Org. Chem.* **2007**, *72*, 6635–6652; b) H. M. D. Bandara, S. C. Burdette, *Chem. Soc. Rev.* **2012**, *41*, 1809–1825; c) M. Irie, T. Fukaminato, K. Matsuda, S. Kobatake, *Chem. Rev.* **2014**, *114*, 12174–12277; d) R. Klajn, *Chem. Soc. Rev.* **2014**, *43*, 148–184; e) S. Wiedbrauk, H. Dube, *Tetrahedron Lett.* **2015**, *56*, 4266–4274; f) I. Aprahamian, *Chem. Commun.* **2017**, *53*, 6674–6684; g) M. M. Lerch, W. Szymański, B. L. Feringa, *Chem. Soc. Rev.* **2018**, *47*, 1910–1937; h) Z. L. Pianowski, *Chem. Eur. J.* **2019**, *25*, 5128–5144.
- [2] D. Villarón, S. J. Wezenberg, *Angew. Chem. Int. Ed.* **2020**, *59*, 13192–13202; *Angew. Chem.* **2020**, *132*, 13292–13302.
- [3] a) G. H. Waldeck, *Chem. Rev.* **1991**, *91*, 415–436; b) M. Oelgemöller, R. Frank, P. Lemmen, D. Lenoir, J. Lex, Y. Inoue, *Tetrahedron* **2012**, *68*, 4048–4056; c) M. Quick, F. Berndt, A. L. Dobryakov, I. N. Ioffe, A. A. Granovsky, C. Knie, R. Mahrwald, D. Lenoir, N. P. Ernsting, S. A. Kovalenko, *J. Phys. Chem. B.* **2014**, *118*, 1389–1402.
- [4] a) T. Shimasaki, S. Kato, K. Ideta, K. Goto, T. Shinmyozu, *J. Org. Chem.* **2007**, *72*, 1073–1087; b) J. F. Xu, Y.-Z. Chen, L.-Z. Wu, C.-H. Tung, Q.-Z. Yang, *Org. Lett.* **2014**, *16*, 684–687; c) S. J. Wezenberg, B. L. Feringa, *Org. Lett.* **2017**, *19*, 324–327; d) Y. Wang, Y. Tian, Y.-Z. Chen, L.-Y. Niu, L.-Z. Wu, C.-H. Tung, Q.-Z. Yang, R. Boulatov, *Chem. Commun.* **2018**, *54*, 7991–7994; e) S. J. Wezenberg, B. L. Feringa, *Nat. Commun.* **2018**, *9*, 1984; f) J. de Jong, B. L. Feringa, S. J. Wezenberg, *ChemPhysChem* **2019**, *20*, 3306–3310; g) J. Sheng, S. Crespi, B. L. Feringa, S. J. Wezenberg, *Org. Chem. Front.* **2020**, *7*, 3874–3879; h) T. S. C. MacDonald, B. L. Feringa, W. S. Price, S. J. Wezenberg, J. E. Beves, *J. Am. Chem. Soc.* **2020**, *142*, 20014–20020; i) D. Villarón, M. A. Siegler, S. J. Wezenberg, *Chem. Sci.* **2021**, *12*, 3188–3193.
- [5] a) J.-F. Xu, Y.-Z. Chen, D. Wu, L. Z. Wu, C. H. Tung, Q.-Z. Yang, *Angew. Chem. Int. Ed.* **2013**, *52*, 9738–9742; *Angew. Chem.* **2013**, *125*, 9920–9924; b) X. Yan, J.-F. Xu, T. R. Cook, F. Huang, Q.-Z. Yang, C.-H. Tung, P. J. Stang, *Proc. Natl. Acad. Sci. USA* **2014**, *111*, 8717–8722; c) F. Xu, L. Pfeifer, S. Crespi, F. K.-C. Leung, M. C. A. Stuart, S. J. Wezenberg, B. L. Feringa, *J. Am. Chem. Soc.* **2021**, *143*, 15, 5990–5997.
- [6] a) Q.-Z. Yang, Z. Huang, T. J. Kucharski, D. Khvostichenko, J. Chen, R. Boulatov, *Nat. Nanotechnol.* **2009**, *4*, 302–306; b) T. J. Kucharski, Z. Huang, Q.-Z. Yang, Y. Tian, N. C. Rubin, C. D. Concepcion, R. Boulatov, *Angew. Chem. Int. Ed.* **2009**, *48*, 7040–7043; *Angew. Chem.* **2009**, *121*, 7174–7177; c) S. Akboulatov, Y. Tian, Z. Huang, T. J. Kucharski, Q.-Z. Yang, R. Boulatov, *Science* **2011**, *357*, 299–303; d) Y. Tian, T. J. Kucharski, Q.-Z. Yang, R. Boulatov, *Nat. Commun.* **2013**, *4*, 2538; e) Z. S. Kean, S. Akboulatov, Y. Tian, R. A. Widenhoefer, R. Boulatov, S. L. Craig, *Angew. Chem. Int. Ed.* **2014**, *53*, 14508–14511; *Angew. Chem.* **2014**, *126*, 14736–14739; f) L. Wang, Y. Yu, A. O. Razgoniaev, P. N. Johnson, C. Wang, Y. Tian, R. Boulatov, S. L. Craig, R. A. Widenhoefer, *J. Am. Chem. Soc.* **2020**, *142*, 17714–17720.
- [7] Y. Li, E. C. M. Tse, C. J. Barile, A. A. Gewirth, S. C. Zimmerman, *J. Am. Chem. Soc.* **2015**, *137*, 14059–14062.
- [8] a) D. Bléger, S. Hecht, *Angew. Chem. Int. Ed.* **2015**, *54*, 11338–11349; *Angew. Chem.* **2015**, *127*, 11494–11506; b) M. Dong, A. Babalhavaei, S. Samanta, A. A. Beharry, G. A. Woolley, *Acc. Chem. Res.* **2015**, *48*, 2662–2670.
- [9] J. Garcia-Amorós, S. Nonell, D. Velasco, *Chem. Commun.* **2012**, *48*, 3421–3423.
- [10] a) R. A. van Delden, N. Koumura, A. Schoevaars, A. Meetsma, B. L. Feringa, *Org. Biomol. Chem.* **2003**, *1*, 33–35; b) L. Pfeifer, M. Scherübl, M. Fellert, W. Danowski, J. Cheng, J. Pol, B. L. Feringa, *Chem. Sci.* **2019**, *10*, 8768–8773.
- [11] S. H. Kawai, S. L. Gilat, R. Ponsinet, J.-M. Lehn, *Chem. Eur. J.* **1995**, *1*, 285–291.
- [12] a) M. Takeshita, C. F. Soong, M. Irie, *Tetrahedron Lett.* **1998**, *39*, 7717–7720; b) C.-T. Poon, W. H. Lam, V. W.-W. Yam, *J. Am. Chem. Soc.* **2011**, *133*, 19622–19625; c) Y. Wu, S. Chen, Y. Yang, Q. Zhang, Y. Xie, H. Tian, W. Zhu, *Chem. Commun.* **2012**, *48*, 528–530; d) S. Wang, X. Li, W. Zhao, X. Chen, J. Zhang, H. Ågren, Q. Zou, L. Zhu, W. Chen, *J. Mater. Chem. C* **2017**, *5*, 282–289.
- [13] a) N. P. M. Huck, B. L. Feringa, *J. Chem. Soc. Chem. Commun.* **1995**, 1095–1096; b) F. Pina, M. João Melo, M. Maestri, R. Ballardini, V. Balzani, *J. Am. Chem. Soc.* **1997**, *119*, 5556–5561; c) G. Szalóki, G. Sevez, J. Berthet, J.-L. Pozzo, S. Delbaere, *J. Am. Chem. Soc.* **2014**, *136*, 13510–13513; d) L. Kortekaas, O. Ivashenko, J. T. van Herpt, W. R. Browne, *J. Am. Chem. Soc.* **2016**, *138*, 1301–1312; e) J. Gurke, Š. Budzák, B. M. Schmidt, D. Jacquemin, S. Hecht, *Angew. Chem. Int. Ed.* **2018**, *57*, 4797–4801; *Angew. Chem.* **2018**, *130*, 4888–4893; f) I. C.-Y. Hou, F. Berger, A. Narita, K. Müllen, S. Hecht, *Angew. Chem. Int. Ed.* **2020**, *59*, 18532–18536; *Angew. Chem.* **2020**, *132*, 18690–18695; g) M. Medved', M. W. H. Hoorens, M. Di Donato, A. D. Laurent, J. Fan, M. Taddei, M. Hilbers, B. L. Feringa, W. J. Buma, W. Szymanski, *Chem. Sci.* **2021**, *12*, 4588–4598.
- [14] a) M. Lohse, K. Nowosinski, N. L. Traulsen, A. J. Achazi, L. K. S. von Krbeek, B. Paulus, C. A. Schalley, S. Hecht, *Chem. Commun.* **2015**, *51*, 9777–9780; b) G. Baggi, L. Casimiro, M. Baroncini, S. Silvi, A. Credi, S. J. Loeb, *Chem. Sci.* **2019**, *10*, 5104–5113.
- [15] a) C. E. Weston, R. D. Richardson, M. J. Fuchter, *Chem. Commun.* **2016**, *52*, 4521–4524; b) A. D. W. Kennedy, I. Sandler, J. Andréasson, J. Ho, J. E. Beves, *Chem. Eur. J.* **2020**, *26*, 1103–1110.
- [16] J. Gurke, M. Quick, N. P. Ernsting, S. Hecht, *Chem. Commun.* **2017**, *53*, 2150–2153.
- [17] M. Jeong, J. Park, S. Kwon, *Eur. J. Org. Chem.* **2020**, 7254–7283.
- [18] Lapouyade and co-workers reported absorption and (time-resolved) emission spectra of (E)-1, full synthetic details were not included: R. Lapouyade, K. Czeschka, W. Majenz, W. Rettig, E. Gilibert, C. Rulliere, *J. Phys. Chem.* **1992**, *96*, 9643–9650.
- [19] Z.-J. Chen, H.-F. Lu, C.-W. Chiu, F.-M. Hou, Y. Matsunaga, I. Chao, J.-S. Yang, *Org. Lett.* **2020**, *22*, 9158–9162.
- [20] For accuracy of TD-DFT, see for example: A. D. Laurent, D. Jacquemin, *Int. J. Quantum Chem.* **2013**, *113*, 2019–2039.
- [21] T. J. Kucharski, R. Boulatov, *J. Mater. Chem.* **2011**, *21*, 8237–8255.
- [22] a) D. S. Noyce, D. R. Hartter, F. B. Miles, *J. Am. Chem. Soc.* **1964**, *86*, 17, 3583–3584; b) D. S. Noyce, D. R. Hartter, F. B. Miles, *J. Am. Chem. Soc.* **1968**, *90*, 17, 4633–4637.
- [23] T. Hao, Y. Yang, W. Liang, C. Fan, X. Wang, W. Wu, X. Chen, H. Fu, H. Chen, C. Yang, *Chem. Sci.* **2021**, *12*, 2614–2622.
- [24] When Et<sub>3</sub>N was added directly to a solution of (E)-1, a similar increase in absorbance was noted (see Figure S24 in the Supporting Information).
- [25] M. Kathan, S. Hecht, *Chem. Soc. Rev.* **2017**, *46*, 5536–5550.

Manuscript received: August 21, 2021

Accepted manuscript online: October 4, 2021

Version of record online: October 21, 2021